International Journal of GEOMATE, Sep., 2024 Vol.27, Issue 121, pp.10-20
ISSN: 2186-2982 (P), 2186-2990 (O), Japan, DOI: https://doi.org/10.21660/2024.121.4073
Geotechnique, Construction Materials and Environment

EVALUATION OF POST-EARTHQUAKE WITH MAGNITUDE OF MW 7.5 IN PALU CITY USING THE PETROGRAPHY, ERT AND CPT

*Hamid Umar[1], Tri Harianto[1], Takenori Hino[2], Ilham Alimuddin[1], Sabrianto Aswad[3] and Sukiman Nurdin[4]

[1]Faculty of Engineering, Hasanuddin University, Makassar, Indonesia;
[2]Department of Civil Engineering and Architecture, Saga University, Japan;
[3]Faculty of Mathematics and Natural Sciences, Hasanuddin University, Makassar, Indonesia;
[4]Faculty of Engineering, Tadulako University, Palu, Indonesia;

*Corresponding Author, Received: 31 July 2023, Revised: 10 July 2024, Accepted: 28 July 2024

ABSTRACT: A critical element in addressing disaster events is conducting a comprehensive study of the phenomenon caused by the disaster (earthquake). Therefore, a comprehensive study of the material from the disaster site, post-disaster handling, and disaster mitigation is needed to understand the phenomenon that occurs. This report presents preliminary results of field monitoring and surveys from several locations affected by the earthquake in Palu on September 28th, 2018, particularly in the Balaroa area and Anutapura Hospital. The purpose of this study is to evaluate the liquefaction potential of earthquake-affected areas using Electrical Resistivity Tomography (ERT) and Cone Penetration Test (CPT). The specific aspect investigated was the condition of the subsoil after the earthquake tested by ERT and CPT. The ERT test result on Trajectories in Balaroa shows the occurrence of a broken aquifer phenomenon, which causes an increase in the water content in the subsoil above it. Smear slides for petrographic investigation were created after the separation of grain sizes. Quartz, biotite, orthoclase, hornblende, plagioclase, and opaque minerals were among the minerals found. The collapse of the Anutapura Hospital building was possibly caused by the presence of local liquefaction phenomena that occurred in some areas of the hospital, which was proven by overlay between CPT and ERT results. Moreover, site investigation by CPT in the disaster area exhibits that soil in particular depth did not reach a non-liquefiable state after an earthquake, indicated by the value of safety factor, and possibly reliquefied for the next earthquake event.

Keywords: Earthquake, Liquefaction, Petrography, Resistivity, Cone penetration test

1. INTRODUCTION

An earthquake is a natural disaster that has an immediate and devastating impact, causing damage to the infrastructure, the earth's terrain, and also casualties. The damage to the infrastructure and the earth's terrain varies depending on the degree of earthquake intensity and the local geological condition. An essential element in responding to a disaster is conducting comprehensive studies related to the phenomena caused by the disaster as study material to understand the phenomenon that happened, post-disaster management, and mitigation in the future.

The Sulawesi island is formed by the collision of terranes from the Australian plate and the Asian plate. Sulawesi Island is a composite island located in the center of the Asia-Australia collision zone [1]. Palu (the capital city of Central Sulawesi Province) is located at 0.53ºS - 119,51ºE and situated at an elevation of 20 meters above sea level. Palu city is surrounded by several active faults, and the Palu-Koro fault (PKF) is considered to be the most active fault in the Palu region [2]. Meanwhile, the PKF is a major strike-slip fault through the center of Sulawesi Island, towards the northern tip of the Matano fault to the south and western part of the Sulawesi Sea, where the north Sulawesi subduction cone is located [3]. According to a previous study [4], the PKF is suspected to be the source of huge earthquakes in Palu City and its surrounding area. The results of research [5] in Palu City show that it is in the high-hazard class in eight sub-districts in Palu City. The earthquake was driven by the super-shear rupture mechanism of the PKF, and this strike-slip movement created the mainshock [6].

The event of an earthquake in Palu City caused casualties and substantial damage, especially in the Petobo and Balaroa districts. The occurrence of large to moderate earthquakes (Mw 6 - 7) in Palu City was also reported by a previous study [7,8,9]. The PKF consists of a series of strike-slip faults that generally NNW-SSE and N-S trends [10]. The prevention of future disasters must clarify the characteristics of damages associated with the activity of the PKF.

The mainshock epicenter of the 2018 Palu earthquake was located approximately 72 km north of Palu city at a depth of 10 km with a coordinate of 0.2559ºS-119.8462ºE. According to geodetic

evidence in the field, the rupture of the fault over a length of 150 km [11]. A massive landslide resulted in the collapse of infrastructures and tsunami waves that hit the coastal area of Palu Bay triggered by the Mw 7.4 earthquake. In general, there are two trends in the rupture zone. The northern part is 80 km through the Donggala district from the epicenter to Palu Bay (North-South trend), while the southern part passes the Palu basin and Sigi Valley (NNW-SSE trend). The impact of the 2018 Palu earthquake was liquefaction and tsunami

This paper presents preliminary monitoring results and surveys of several earthquake-affected locations in the city of Palu on September 28th, 2018, such as in the Balaroa area and Anutapura Hospital. These two areas were chosen as the study because they suffered the most damage. A study of soil shear strength by cone penetration test (CPT) at Anutapura Hospital and a comparison with it before the 2018 earthquake event was reported in this paper. Furthermore, this study also describes that CPT results could be used to evaluate the potential for an earthquake to trigger cyclic liquefaction. Moreover, this study also discusses post-liquefaction data collection and analysis by CPT to identify the potential of re-liquefiable sites.

2. RESEARCH SIGNIFICANCE

This research focuses on soil resistivity analysis using Electrical Resistivity Tomography (ERT) and Cone Penetration Test (CPT). The ERT test is very important to describe subsurface conditions that have complex or irregular geology. The CPT test is carried out by measuring the cone resistance at each depth until it reaches hard soil, then analyzing the CPT test before and after the earthquake to determine changes in the soil layer. This research also combines ERT and CPT data into one unit in the analysis, making it easier for planners to mitigate the possibility of disaster due to future earthquakes.

3. METHODS

3.1 Electrical Resistivity Tomography (ERT)

Electrical resistivity tomography, known as ERT, was widely used to obtain two-dimensional (2-D) and three-dimensional (3-D) subsurface images based on high-resolution resistivity values [13-15]. The 2-D and 3-D imaging are crucially essential to image the subsurface condition that has complex or irregular geology. In this study, excellent geomative tools were used with the configuration of Wenner Schlumberger, with a total of 60 pieces of electrodes. The configuration is used because it has good sensitivity to see the vertical cross-section of the subsurface model. Spaces of electrode distance vary from 4 to 5 meters, adjusted according to the length of the track and the number of electrodes. A trajectory was located in the Balaroa area with an electrode spacing of 5 meters and other tracks with a space of 4 meters, located at Anutapura Hospital, as shown in Figure 2. The position of the Palu Koro Fault is in the middle, between the location of Balaroa and the location of Anutapura Hospital.

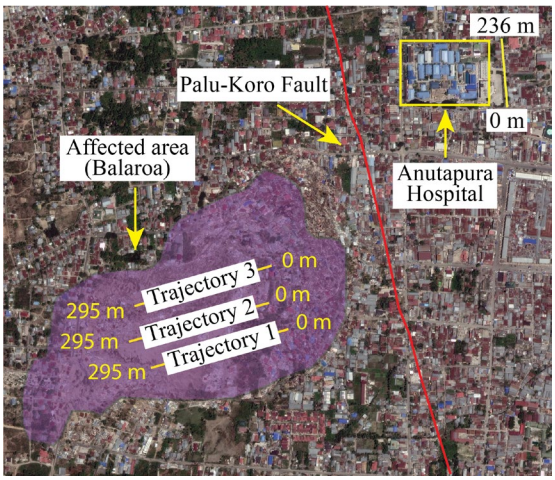

Fig.1 Trajectory of 2-D Electrical Resistivity Tomography

The resistivity image was obtained using the RES2DINV program for automatic 2-D inversion of the apparent resistivity obtained in the field. The inversion scheme is based on the least square method with smoothness constraints with quasi-Newton optimization. The optimization of the iteration process is adjusted until the difference between the measurement data in the field (observation), and the calculation model of the apparent resistivity values are as minimal as possibly indicated by the value of the smallest root mean squared (RMS).

3.2 Cone Penetration Test (CPT)

The soil investigation through the Cone Penetration Test (CPT) was conducted around the Anutapura hospital (coordinate of 0°54'0.14" South Latitude – 119°50'58.37" East Longitude). The CPT test follows the American Standard Testing and Materials (ASTM D-3441). The CPT test location at Anutapura Hospital is about 200 m from the Palu-Koro fault. The CPT provides continuous penetration resistance profiles, which are useful for identifying soil stratigraphy and providing a preliminary estimation of liquefaction potential in

sandy soil. In recent years, there has been an increase in available field-testing data including CPT [16]. The CPT test was conducted by measuring the cone resistance at each depth until reached the hard soil. Furthermore, the analysis of CPT test results before and after an earthquake was obtained to investigate the change in the soil layer post-earthquake.

An approach for estimating the possibility of cyclic liquefaction caused by seismic loads was devised by Seed et al [17]. This method requires the estimation of the ground's cyclic resistance ratio (CRR) and the cyclic stress ratio (CSR) profile brought on by the design earthquake. If the CRR is less than the CSR, cyclic liquefaction may take place. The CSR value is often calculated using the earthquake's probability of occurrence. Additionally, Seed and Idriss [18] created the following straightforward technique to calculate CSR based on the site's highest ground surface acceleration (amax) at the site as follows:

$$CSR = \frac{\tau_{av}}{\sigma'_{vo}} = 0.65\left[\frac{a_{max}}{g}\right]\left(\frac{\sigma_{vo}}{\sigma'_{vo}}\right) r_d \quad (1)$$

Where τ_{av} is the average cyclic shear stress; g is the acceleration due to gravity (9,81 m/s^2); a_{max} is the maximum horizontal acceleration at the ground surface; σ_{vo} and σ'_{vo} are the total and effective vertical overburden stresses and r_d is a stress reduction factor which is dependent on depth. The factor r_d can be estimating using the bi-linier function at every depth (z), as presented in equations 2 and 3.

$$r_d = 1.0 - 0.00765z \quad (\text{if } z < 9.15 \text{ m}) \quad (2)$$

$$r_d = 1.174 - 0.0267z \quad (\text{if } z = 9.15 - 23 \text{ m}) \quad (3)$$

Furthermore, Seed et al. [17] also developed a method to estimate the cyclic resistance ratio (CRR) for clean sand. Robertson and Campanella [19] reported that the existing CPT-based correlation for clean sand is generally good and can be estimated using the following equations (Mw 7.5):

$$\boldsymbol{CRR_{7.5} = 93\left[\frac{(q_{c1N})_{cs}}{1000}\right]^3 + 0.08}$$

$$(\text{if } 50 \leq (\boldsymbol{q_{c1N}})_{cs} \leq 160) \quad (4)$$

$$\boldsymbol{CRR_{7.5} = 0.833\left[\frac{(q_{c1N})_{cs}}{1000}\right] + 0.05}$$

$$(\text{if } (\boldsymbol{q_{c1N}})_{cs} < 50) \quad (5)$$

Robertson and Wride [16] suggest estimation the equivalent sand normalized cone penetration resistance $(\boldsymbol{q_{c1N}})_{cs}$ as presented in Equation 6. Correction factor (K_c) is a function of soil grain characteristics, $\boldsymbol{q_c}$ is cone resistance, and $(\boldsymbol{q_{c1N}})$ is the normalized CPT penetration resistance. The value of K_c is assumed to be 1.0 for clean sand to silty sand and *n* value is 0.5.

$$(\boldsymbol{q_{c1N}})_{cs} = \boldsymbol{K_c}(\boldsymbol{q_{c1N}}) \quad (6)$$

$$\text{where} \quad (\boldsymbol{q_{c1N}}) = \frac{(q_c - \sigma_{vo})}{100}\left(\frac{100}{\sigma'_{vo}}\right)^n \quad (7)$$

Moreover, the factor of safety (SF) against liquefaction is defined as (this study using the magnitude of earthquake, Mw = 7.5):

$$\boldsymbol{FS = \frac{CRR_{7.5}}{CSR}\, MSF} \quad (8)$$

where MSF is the magnitude Scaling Factor.

Youd et al. [12] recommend that the value of MSF is equal to 1 for Mw = 7.5. The liquefaction phenomenon often occurs in multiple layers, which can only be observed in the complete CPT data profile. Therefore, this study conducted the safety factor analysis up to hard soil.

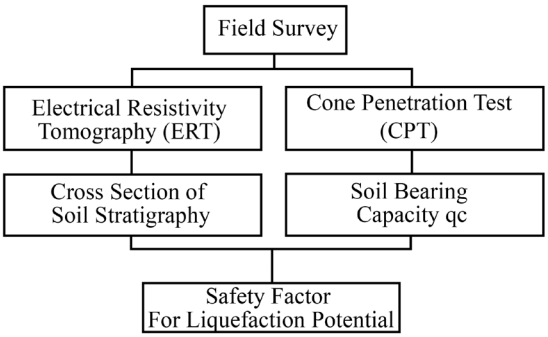

Fig.2 Flowchart of Research Method

4. RESULTS AND DISCUSSION

4.1 Characteristics of Soil Layers Based on Two-Dimension (2d) Electrical Resistivity Tomography

4.1.1 Balora Area

The topography of the affected area in Balaroa was identified as a gentle slope with an inclination of 1-3%. According to the witnesses, the ground surface was undulating during the earthquake and subsequently, a mudflow appeared and pushed the houses down to the lower elevation.

Figure 3 shows the resistivity cross-section of trajectory 1 obtained from 12 iterations with an RMS error value of 1.5%. This resistivity cross-section reaches a depth of 57.4 meters with a resistivity range value of 20.53 - 165 Ωm. Resistivity values of 20.53 - 35.6 μm in shallow

aquifer layers with depth distribution ranging from 1.25 - 13 meters and intermediate aquifers with resistivity values of 35.6 - 58.2 Ωm with depths ranging from 19 - 28 meters.

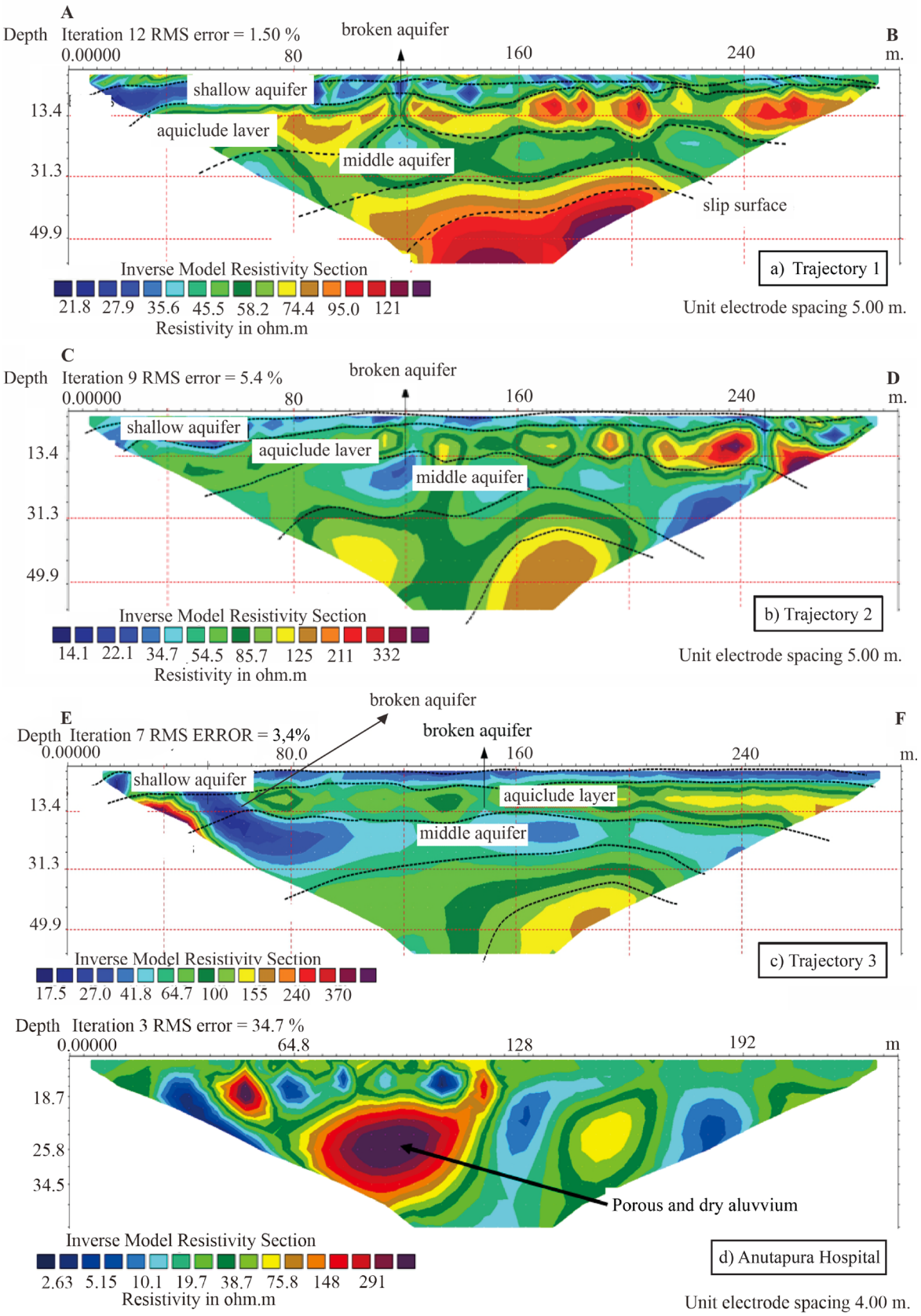

Fig.3 Cross-section profile ERT in Balaroa area of (a, b, c) and in Anutapura Hospital area of (d)

Between the two layers is the aquiclude layer, a layer that can store water but cannot deliver significant amounts of water. The aquiclude layer is located at depths ranging from 8 meters - 25 meters with resistivity values of 64.7 - 155 Ωm. Also, the slip plane can be identified, marked by the contrast resistivity seen at the bottom. Furthermore, it can also be predicted slip fields marked by resistivity contrast seen at the bottom (between red and yellow). At this location, it was also found the phenomenon of a ruptured aquifer that caused increased water content in the soil layers above. This phenomenon is an indicator of increasing liquefaction potential in this area.

The resistivity cross-section obtained from 9 iterations, with an RMS error value of 5.4%, is shown in Figure 3. The resistivity cross-section reaches a depth of 57.4 meters, with a resistivity range of 12.58 - 583.36 Ωm. Resistivity values of 14.1 - 34.7 µm in shallow aquifer layers with depth distribution ranging from 1.25 - 12 meters and intermediate aquifers with resistivity values of 22.1 - 54.5 µm with depths from 15 - 30 meters. Between the two layers is the aquiclude layer, a layer that can store water but cannot deliver significant amounts of water. This aquiclude layer is at a depth of around 6 meters - 20 meters with resistivity values of 125 - 639.07 Ωm. In addition, it can also be estimated that the slip plane is marked by the resistivity contrast seen at the bottom.

The resistivity cross-section obtained from iteration 7, with an RMS error value of 3.4% for trajectory three, is shown in Figure 3. This resistivity cross-section reaches a depth of 57.4 meters with a resistivity range value of 15.68 - 639.07 Ωm. Resistivity values of 17.5-27 Ωm in shallow aquifer layers with depth distribution ranging from 1.25 - 9 meters and medium aquifers with resistivity values of 17.5 - 41.8 Ωm with depths ranging from 18 - 33 meters. Between the two layers is the aquiclude layer, a layer that can store water but cannot deliver significant amounts of water. This aquiclude layer is at a depth of around 7 meters - 17 meters.

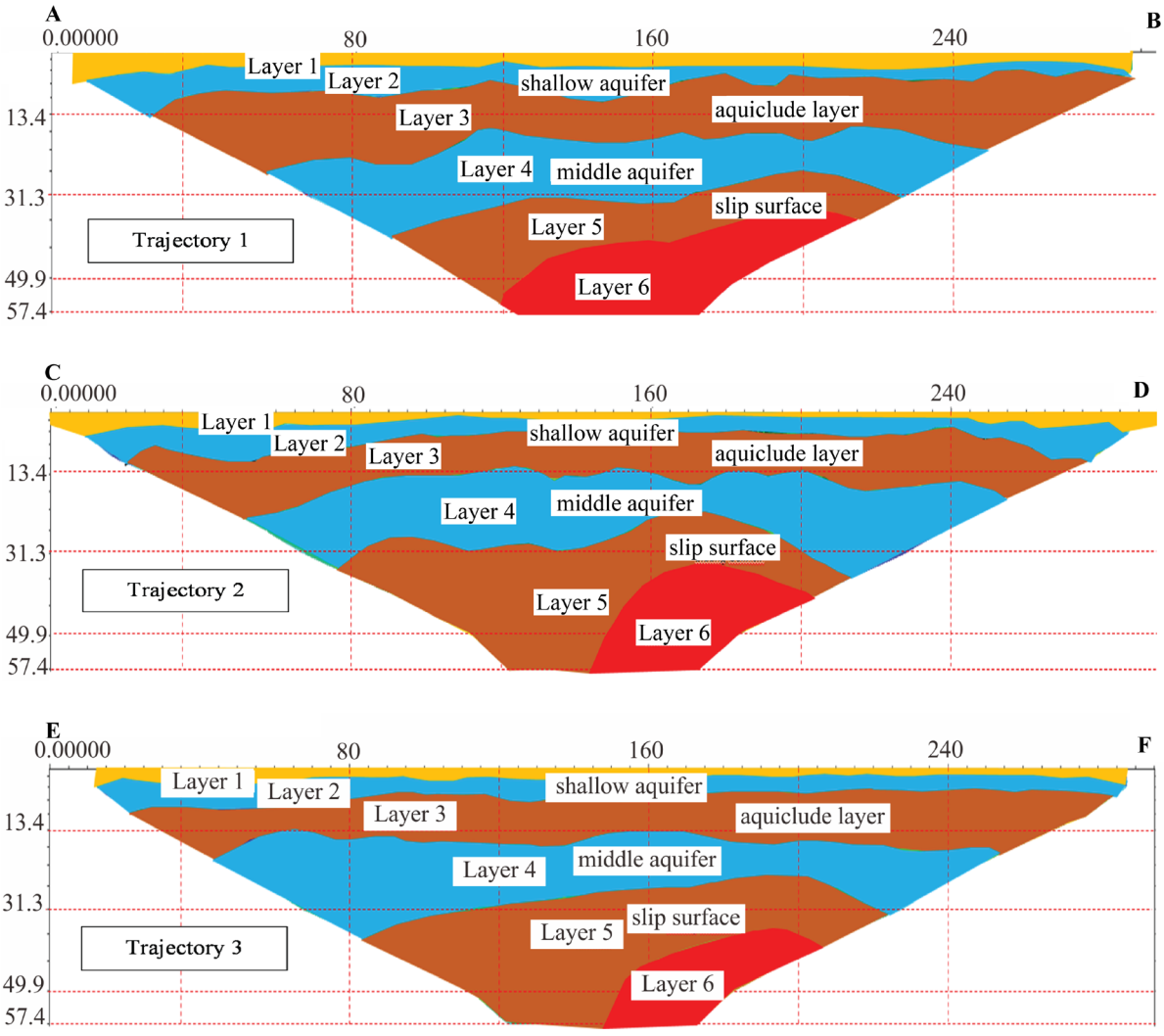

Fig.4 Soil stratigraphy results from resistivity test

Furthermore, it can be predicted slip fields marked by resistivity contrast observed at the bottom of the soil layer resulting from the interpretation of resistivity.

The resistivity values and patterns obtained from the cross-section (trajectory 1 to 3), the geology soil profile of the cross-section can be predicted, as shown in Figure 4. Based on the interpretation of the resistivity test results, six different layers can be predicted, namely layer 1 is clay (clay) to the lump (boulder). Layer 2 is sand and silt with some clay. Layer 3 is a layer of clay, silt, or rock. Layer 4 is sandy soil. Layer 5 is dominated by clay. Layer 6 is bedrock (this layer is a group of metamorphic or granite rock metamorphic or granite).

An important finding was collected from the Balaroa area. A broken aquifer phenomenon was found in the disaster area as shown in Figure 4, and this broken aquifer causes an increase in water content in the soil layer above it. This phenomenon is one indicator that contributed to increasing the potential of liquefaction in this area. The substantial lateral movement of the ground after an earthquake is suspected to be caused by the loose sand soil layer (generally 0-15 m) saturated by water leakage from a broken aquifer and subsequently subjected to vibration (earthquake), which led to liquefaction

4.1.2 Anutapura Hospital Area

The electrical resistivity tomography (ERT) test was carried out at the location around the Anutapura Hospital. The test track is conducted along the existing street (Tolambu Street), as shown in Figure 1. The starting point of the ERT measurement at this location is at the coordinates of 0°54'2.57" South Latitude and 119°50'59.95" East Longitude.

Figure 3 shows a cross-section of the ERT test results with a depth of up to 45.9 meters, and the value of resistivity ranging from 2.22 - 673.97 Ωm. The porous and dry alluvium is identified at a depth ranging from 17.0 to 31.0 meters. The ERT test result also shows the presence of sand and silty sand at a depth of around 2-3 meters, and the water table level is very high (near the surface). This combination during an earthquake could cause the phenomenon of liquefaction.

4.2 Minerals Area

The difference in the area ratio of minerals in the liquefaction zone and the non-liquefaction zone is an indicator to determine the occurrence of pressure and friction between grains at the time of liquefaction. It can be distinguished under normal conditions from the sedimentation process in the form of distance and time of transportation, strength, and magnitude of the flow and size and shape of the minerals [27].

This mineral area calculation is measured by calculating the area from the smallest to the largest minerals in the same mineral for each sample both in the Liquefaction Zone (LZ) and Non-Liquefaction Zone (NLZ) as shown in Figure5. These results indicate that of the mineral area in the liquefaction zone is smaller than in the non-liquefaction zone. It is also found that the mineral area that has a small size is less resistant or less stable minerals, especially pyroxene minerals, which show clear and significant differences in the three locations both in the liquefaction zone and the non-liquefaction zone. Grain size, and especially quartz size, must also be considered in these analyses since the tests demonstrated that larger grains break at higher stresses than finer grains.

Figure 5 shows the size and shape of minerals that are smaller in the liquefaction area and the percentage of minerals that are damaged, cracked, and broken is higher, resulting in weakened soil strength.

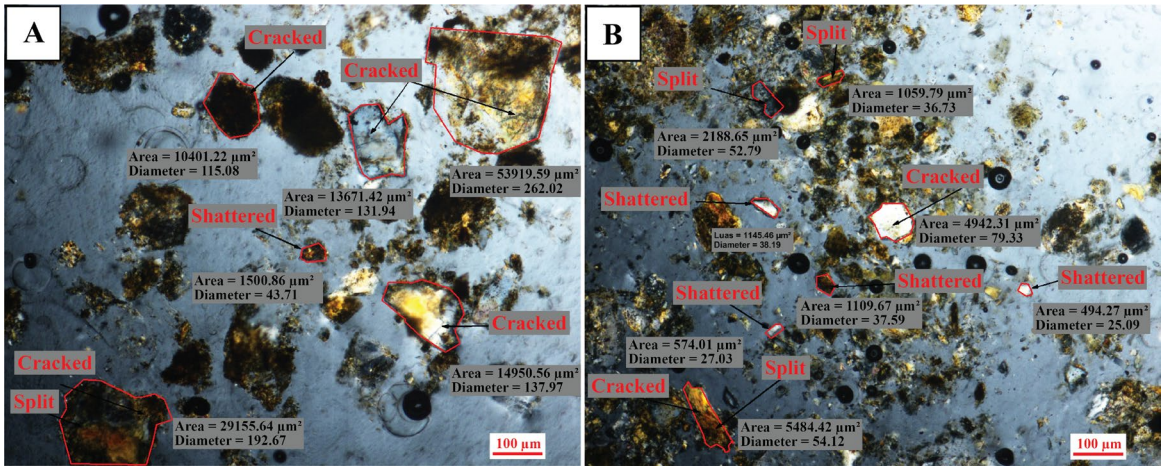

Fig.5 Photomicrograph in cross-polarized showed comparison of mineral condition, (A) Balaroa liquefaction zone (B) Balaroa non-liquefaction zone

4.3 Soil Profile Change Post-earthquake

The condition of the Anutapura Hospital building that was damaged by the earthquake can be seen in Figure 6. The building suffered a partial collapse in which part of the building experienced a horizontal shift (around 6 m) and, at the same time, experienced a collapse on the floor and basement. Figure 7 shows the detailed collapse pattern of the hospital building. The collapsed building separated from the main building, and structural failure was found in ruins. The soil investigation through the Cone Penetration Test (CPT) was conducted around the Anutapura Hospital).

Analysis of CPT results before and after an earthquake was conducted to investigate the change in the soil layer. The values of the cone resistance with depth are presented in Figure 7. The value of cone resistance taken before the earthquake (12 September 2016), is shown in Figure 7(a). The type of subsoil based on the CPT results is determined using the Robertson chart by correlating the cone resistance and the friction ratio [20-22].

The soil profile was dominated by loose sandy silt up to 3 m with a high water table (1.5m), extended depth of the soil profile varied between sand and sandy silt. During an earthquake loading, loose sand experiences large shear strains, which could result in a large vertical and horizontal deformation.

The deformation types depend on the ground geometry (e.g., embankments, slopes, buildings, etc.) and external loads. Very loose sand can also experience loss in strength during an earthquake, which can result in flow slides with extensive deformations depending on the drainage and ground geometry. The presence of saturated loose sandy soil in this investigation site possibly caused liquefaction, especially when the soil layer is subjected to an earthquake.

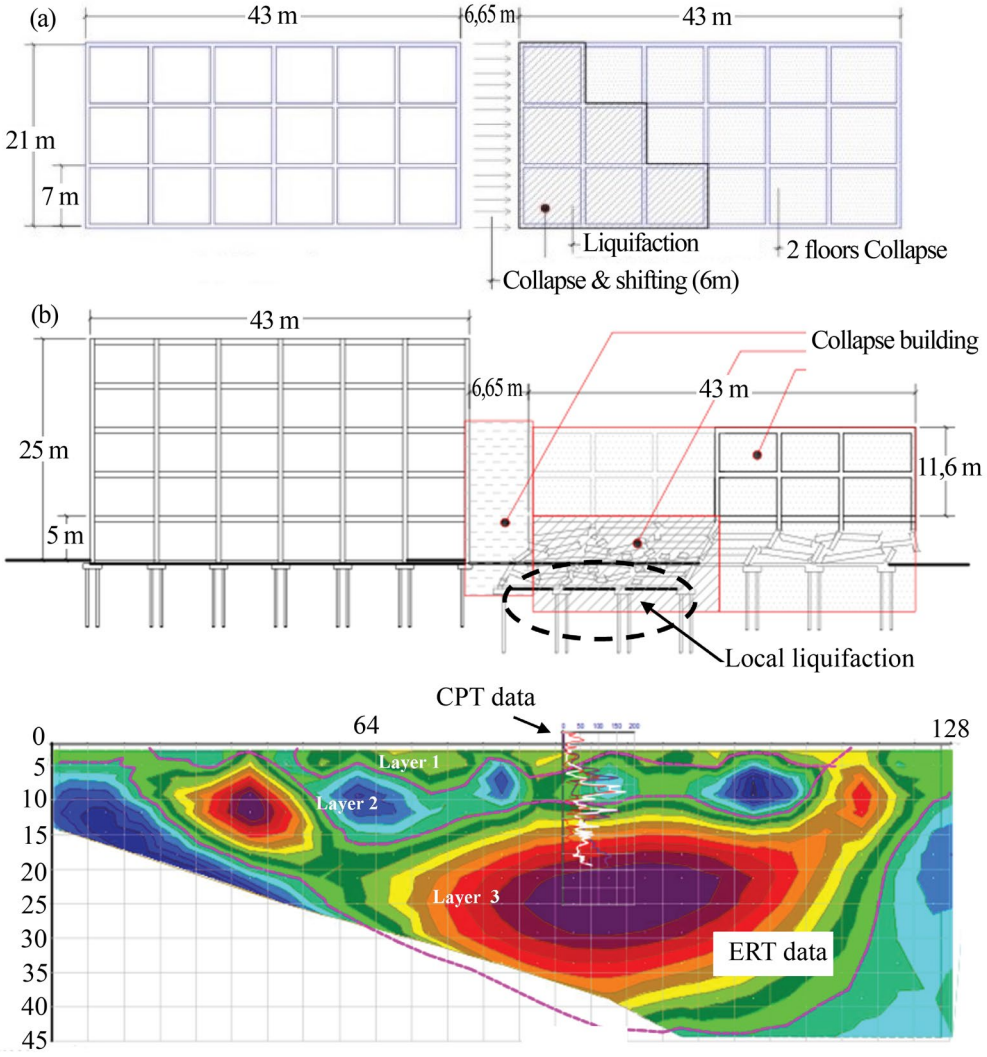

Fig.6 Schematic detail of hospital building collapse (a) upper view, (b) front view, and illustration of possibly local liquefaction phenomenon in Anutapura

The partial collapse of the Anutapura Hospital building due to local liquefaction phenomena is revealed by the data collected from CPT. One way to analyze liquefaction is to use CPT data. CPT data can be collected with simple equipment. By calculating the safety factor using CPT data, it is useful to know the potential for liquefaction recurrence in the same location.

Figure 7(b) shows the significant changes in cone resistance values from the CPT results after an earthquake (2 December 2018). In-depth near the surface (0-3 meters), there was a significant increase in cone resistance value due to the soil layers' compression. Moreover, variations in the cone resistance values are found in the deeper soil layer. Increasing the cone resistance and density observed in some depth of the soil layers after the event of an earthquake. Generally, the compressed soil experienced an increase in soil shear strength [23].

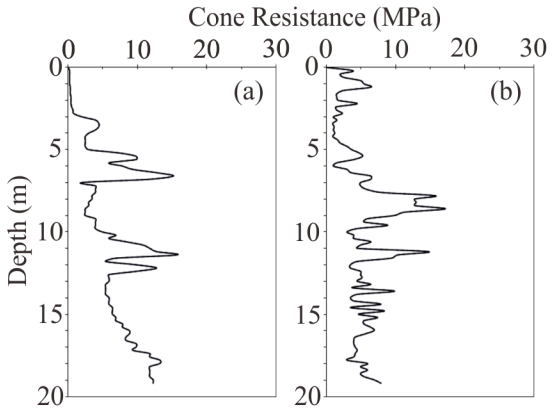

Fig.7 Variation of CPT profile before and after an earthquake in Anutapura Hospital (a) before an earthquake and (b) after an earthquake

To obtain a comprehensive analysis of the changes in soil conditions at a certain depth, the ERT test was also carried out at the location near the CPT location. The subsoil profile results from the ERT test and CPT was then plotted to verify the type of subsoil after experiencing an earthquake, as shown in Figure 6. The result of the resistivity (ERT) test is shown and explained in the previous section. The ERT and CPT test results indicated that the subsoil beneath the Anutapura Hospital building structure was dominated by granular material layers such as sand, silty sand, and sandy silt, classified as highly liquefiable soil. Figure 8 shows the plot data between the ERT and CPT profiles. Liquefaction-induced ground settlements are mostly vertical deformations of surficial soil layers caused by the densification of loose granular soils following earthquake loading. Moreover, the soil profile from post-earthquake CPT data showed the hardening layers tendency in some depth.

Following earthquake loading, sandy soils experienced volumetric strain and post-earthquake settlement. It is general knowledge that a site that experienced liquefaction and soil reached a denser state that could not be liquefied (non-liquefiable) in a future earthquake event. However, some cases reported that after an earthquake, the soil did not reach a non-liquefiable state and revealed that some sites were re-liquefied during the earthquake event [24]. Therefore, in the next section, the cyclic liquefaction potential analysis using this site's CPT data will be discussed.

4.4 Cyclic Liquefaction Potential using the CPT Data

Under earthquake loading, the soil generally deforms. Cyclic loading is rapidly imposed by earthquakes and soil responds to undrained conditions during earthquakes. Soils developed pore pressure during earthquake loading, and at small strains, these pore pressures are almost always positive. Sand-like soils can develop high positive pore pressures during undrained cyclic loading and can reach a condition of zero effective confining stress. At zero effective stress, the soil loses its initial structure, the stiffness of the soil in shear is essentially zero or very small, and large deformations can occur during earthquake loading. The condition of zero effective stress is often defined as liquefaction or cyclic liquefaction [25].

Evaluation of the cyclic liquefaction of the post-liquefied CPT data of the Anutapura hospital site according to Youd et al. [12]. The value of amax/g = 0.4 [26]. was taken for the analysis, and Mw is chosen 7.5. It has been common to adopt an earthquake magnitude M = 7.5, effective overburden stress of s'vo = 1 atm [25]. The results of the CPT method to evaluate cyclic liquefaction is shown in Figure 9.

The advantage of the CPT-based liquefaction method is that a continuous factor of safety (FS) profile against liquefaction can be obtained. In-depth near the surface (0.5 – 1.5m), the soil tends to be in a non-liquefiable state indicated by the value of FS >1. Continuously, the non-liquefiable layer is also found in the depth of 7.5 - 9 m, in line with the increasing of the cone resistance value. Generally, it is found that the layer that is assumed to be non-liquefiable (FS >1) after an earthquake increases in some depths.

The CPT-based method described previously, provides a continuous profile of FS value for a given design earthquake loading as shown in Figure 16. The main advantage of the method of CPT-based liquefaction is that continuous profiles can be calculated rapidly, which allows the engineer to analyze the profile in detail and apply engineering judgment for future construction.

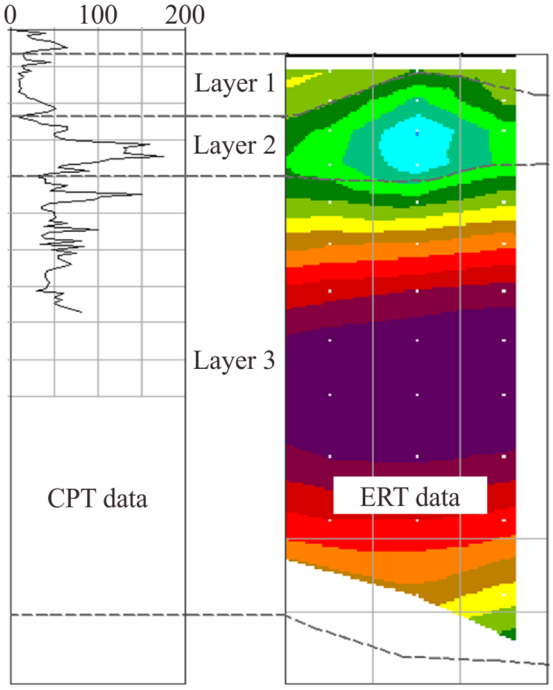

Layer	Depth (m)	Tip resistance qc (kg/cm2)	Soil type	Resistivity (10^3 Ω meter)
Layer 1	1.00 - 5.80	9 - 65	Sandy silt	19.7
				38.7
				75.8
Layer 2	5.80 - 10.20	10 - 175	Sand	2.63
				5.15
				10.1
				19.7
Layer 3	10.20 - 40.60	30 - 150	Silty Sand	75.8
				148
				291

Fig.8 Plotted data between CPT and ERT profile

The CPT-based method described previously, provides a continuous profile of FS value for a given design earthquake loading as shown in Figure 9. The main advantage of the method of CPT-based liquefaction is that continuous profiles can be calculated rapidly, which allows the engineer to analyze the profile in detail and apply engineering judgment for future construction. The CPT-based liquefaction method is a simplified approach and is hence conservative. This liquefaction evidence could be used as valuable information for the stakeholders in designing more disaster-resistant buildings in the future. By using CPT analysis we can predict the potential for liquefaction in the future in the event of an earthquake. The analysis used is simple enough that it can be used easily. The results of this study can be used by planners to design buildings that are resistant to liquefaction in the event of a future earthquake.

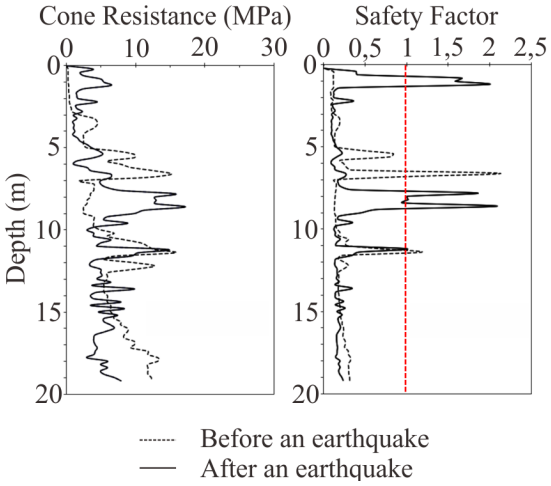

Fig.9 Post-earthquake evaluation of cyclic liquefaction

5. CONCLUSION

Based on the results of the analysis from this field investigation and survey, several phenomena have been identified at the study locations, including:

1. This study can evaluate the liquefaction potential of earthquake-affected areas using Electrical Resistivity Tomography (ERT) and Cone Penetration Test (CPT).
2. In this study, radar satellite imagery (SAR) is used to show changes in surface profiles before and after an earthquake. In the intensity image, it is observed surface objects that have undergone changes based on the characteristics of the object being observed.
3. The mineral area in the liquefaction zone is smaller than in the non-liquefaction zone. In liquefaction zones the percentage of damaged, cracked, and broken minerals is higher, resulting in weakened soil strength.
4. The resistivity test result on 3 trajectories in the Balaroa area shows the occurrence of a broken aquifer phenomenon, which causes an increase in the water content in the subsoil above it. This phenomenon is one indicator of the causes of liquefaction in this area.
5. The result of the CPT and resistivity test shows that the subsoil beneath the collapsed structure of the Anutapura Hospital building is dominated by layers of sand, sandy silt, and silty sand. The collapse of the Anutapura Hospital building was caused possibly by the presence of local

liquefaction phenomena that occurred in some areas of the hospital, which was proven by overlay between CPT and resistivity results. CPT data analysis is one method for liquefaction analysis. It is helpful to know the possibility of liquefaction recurrence in the same location by calculating the safety factor using CPT data.

6. By combining ERT and CPT data into one unit in the analysis, it is easier for planners to mitigate the possibility of disaster due to earthquakes in the future.
7. It is general knowledge that a site that experienced liquefaction and soil reached a denser state that could not be liquefied in a future earthquake event. However, site investigation in the disaster area exhibits that soil in particular depth did not reach a non-liquefiable state indicated by the value of safety factor and potentially re-liquefied during aftershocks. The recommendations from this research can be used by relevant agencies in issuing earthquake-resistant building regulations.

6. ACKNOWLEDGMENT

The authors received no financial support for the investigation, authorship, and publication of this study.

7. REFERENCES

[1] Von Rintelen T., Stelbrink B., Marwoto R. M., and Glaubrecht M., A Snail Perspective on the Biogeography of Sulawesi, Indonesia: Origin and Intra-Island Dispersal of the Viviparous Freshwater Gastropod Tylomelania, PLOS ONE, Vol. 9, No. 6, 2014, pp. 1-11.

[2] Irsyam, M,, Widiyantoro, S., Natawidjaja, D. H., Meilano, I., Rudyanto, A., Hidayati, S., Triyoso, W., Hanifa, N. R., Asrurifak, M., Ridwan, M., Cummins, Philr., Faizal, L. and Syahbana, A. J., Development of the 2017 national seismic hazard aps of indonesia, Earthquake Spectra, Vol. 36, Issue 1, 2017, pp. 112-136.

[3] Hamilton, W., Tectonics of the Indonesian region, US Geological Survey Professional Paper, 1979, pp. 1-345.

[4] Bao, H., Ampuero, J. and Meng, L. (2019). Early and persistent supershear rupture of the 2018 magnitude 7.5 Palu earthquake, Nat. Geosci, Vol. 12, No. 3, 2018, pp. 200-205.

[5] Rusydi, M., Efendi, R., Sandra and Rahmawati, Earthquake hazard analysis use Vs30 data in Palu, Journal of Physics: Conference series, Vol. 979, 2017, pp. 1-10.

[6] Socquet, A., Hollingsworth, J. and Pathier, E., Evidence of supershear during the 2018 magnitude 7.5 Palu earthquake from space geodesy, Nat. Geosci, Vol 12, No. 3, 2019, pp. 192-199

[7] Prasetya, G. S., de Lange., W. P., and Healy, T. R., The Makassar strait tsunamigenic region, Indonesia., Nat. Hazards, Vol. 24, 2001, pp. 295-307.

[8] Gomez, J. M., Madariaga, R., Walpersdorf, A., and Chalard, E., The 1996 earthquakes in Sulawesi, Indonesia., Bull Seismol. Soc. A., Vol. 90, No. 3, 2000, pp. 739-751.

[9] Pelinovsky, E., Yuliadi, D., Prasetya, G. and Hidayat, R., The 1996 Sulawesi tsunami, Nat. Hazards, Vol. 16, 1997, pp. 29-38.

[10] Bellier, O., Sebrier, M., Beaudouin, T. H., Villeneuve, M., Braucher, R., Bourles, D., Siame L., Putranto, E, Pratomo, I., High Slip rate for a low seismicity along the Palu-Koro active fault in central Sulawesi (Indonesia), Terra Nova, Vol. 13, No. 6, 2001, pp. 463-470.

[11] Geotechnical Extreme Events Reconnaissance (GEER), Geotechnical Reconnaissance: the September 28 2018 M7.5 Palu-Donggala, Indonesia earthquake, Geotechnical Extreme Events Reconnaissance Association, 2019, pp. 1-77

[12] Youd, T. L., Idriss, I. M., Andrus, R. D., Arango, I., Castro, G., Christian, J. T., Dobry, R., Finn, W. D. L., Harder, L. F., Hynes, M. E., Ishihara, K., Koester, J. P., Liao, S. S. C., Marcuson, W. F., Martin, G. R., Mitchell, J. K., Moriwaki, Y., Power, M. S., Robertson, P. K., Seed, R. B., and Stokoe, K. H., Liquefaction resistance of soils: Summary report from the 1996 NCEER and 1998 NCEER/NSF Workshops on Evaluation of Liquefaction Resistance of Soils, Journal of Geotechnical and Geoenvironmental Engineering, Vol. 127, Issue 10, 2001, pp. 817-833.

[13] Gunther, T, and Rucker, C., Electrical Resistivity Tomography (ERT) in geophysical application – state of the art and future challenges, 100 Years of Electrical Imaging, Vol. 1, Issue 5, 2012, pp. 33-36.

[14] Ungureane, C, Priceputu, A, Bugea, A. L, and Chirica A, Use of electric resistivity tomography (ERT) for detecting underground voids on highly anthropized urban construction sites, Procedia Engineering, Vol. 209, 2017, pp. 202-209,

[15] Oldenborger, G.A, Routh, P.S., and Knoll M.D, The sensitivity of electrical resistivity tomography data to electrodeposition errors, Geophysical journal international, Vol. 162, Issue 1, 2005, pp. 1-9.

[16] Robertson, P. K. and Wride, C. E., Evaluating cyclic liquefaction potential using the CPT,

Canadian Geotechnical Journal, Vol. 35, No. 3, 1998, pp. 442-459.

[17] Seed, H. B., Tokimatsu, K., Harder, L. F. and Chung, R. M., Influence of SPT procedures in soil liquefaction resistance evaluations, Journal of Geotechnical Engineering, ASCE, Vol. 111, Issue 12, 1985, pp. 1425-1440.

[18] Seed, H. B. and Idriss, I. M., Simplified procedure for evaluation soil liquefaction potential, Journal of the Soil Mechanics and Foundations Division, ASCE, Vol. 97, Issue 9, 1971, pp. 1249-1273.

[19] Robertson, P. K. and Campanella, R. G., Liquefaction potential of sand using the cone penetration test, Journal of Geotechnical Engineering, ASCE, Vol. 22, Issue 3, 1985, pp 298-307.

[20] Thein, P.S., Pramuwijoyo, S., Brotopuspito, K. S., Kiyono, J., Wilopo, W., Furukawa, A. and Setianto, A., Estimation of seismic ground motion and shaking parameters based on microtremor measurements at Palu city, Central Sulawesi province, Indonesia., World Academic of Science, Engineering and Technology, International Journal of Geological and Environmental Engineering, Vol. 8, No. 5, 2014, pp. 308-319.

[21] Robertson, P.K., Soil classification using the cone penetration test, Canadian geotechnical journal, Vol. 27, No. 1, 1990, pp. 151-158

[22] Lunne, Tom, Robertson, Peter K & Powel John J.M., Cone penetration testing in geotechnical practice, Chapman & Hall, London, UK, 1997, pp. 1-305

[23] Robertson, P.K., Evaluating soil liquefaction and post-earthquake deformations using the CPT, Geotechnical and Geophysical Site Characterization, v.1, (Proceedings ISC-2, Porto), Millpress, Rotterdam, Vol. 2, 2004, pp. 233-249

[24] Rahman, M and Thallak, S.G., Post-liquefaction data collection and analyses for an earthquake in New Zealand, Proceedings of 4th International seminar forensic geotechnical engineering, Bengaluru, India, 2015, pp 241-253.

[25] Robertson, P.K., Performance based earthquake design using the CPT, Proceedings of the International Conference on Performance-based Design in Earthquake Geotechnical Engineering (IS-Tokyo), 2009, pp. 1-21

[26] Pradoto, R.G.K., Oktavianus, A., Pribadi, K.S, Rasmawan, I.M.A.B, Wulandari L.D., Palu Housing Reconstruction Process: Reviewing and Learning after the 2018 Earthquake, IOP Conf. Series: Earth and Environmental Science, Vol. 1065, pp. 1-15

[27] Umar, H., Irfan, U.R., Sahabuddin, Cakrawal, M. S., The effect of liquefaction on mineral breakage physical in the Palu city, Central Sulawesi province, Indonesia., IOP Conf. Series: Earth and Environmental Science, Makassar, Indonesia., Vol. 1134, 2021, pp. 1-10